

Real-time Modified PID Controller over a DC-DC Boost Converter

Eduardo Giraldo

Abstract—A Hardware-In-the-Loop evaluation of a modified PID controller applied over a DC-DC Boost Converter is presented. The controller is designed by considering a linearized representation of the system, validated in real-time over an embedded system. The controller's design is performed by considering the operation of the closed-loop system around the equilibrium point. The proposed method considers a settling time approach for a transfer function of a non-minimum phase system. Also, the proposed approach is validated for simulated and real-time systems under a Hardware-In-the-Loop structure. The closed-loop system is evaluated for time-varying loads (parametric disturbances) and external disturbances. As a result, the proposed approach effectively achieves the design criteria in terms of settling time. In addition, the tracking performance of the proposed approach is evaluated for step and impulse reference signals in real-time by using the Hardware-In-the-Loop structure.

Index Terms—Real-time, PID control, Boost converter.

I. INTRODUCTION

THE implementation of real systems by using Hardware-In-the-Loop (HIL) or Software-In-the-Loop (SIL) structures is nowadays the most common approach to evaluate the effectiveness of the controller over nonlinear systems [1]. For non-complex linear systems, the implementation by using analog computation is always an option [2], [3], but this method requires a lot of resources when the complexity of the system is increased [4], and for that reason, HIL and SIL approaches are now the gold standards for real-time simulation.

DC-DC Buck and Boost converters are the nonlinear systems most used in power electronics applications [5]. Several controllers can be designed to fulfill the closed-loop requirements, as proposed in [6], where a nonlinear controller for a Buck converter is presented, or in [7], where a passivity-based control is designed for a Buck-Boost converter. It is worth noting that the evaluation of the controller's performance over these systems is developed by using HIL or SIL structures [8], [9], or by using a very low-cost real-time simulation environment [10].

In this work, a Hardware-In-the-Loop evaluation of a modified PID controller applied over a DC-DC Boost Converter is presented. The controller is designed by considering a linearized representation of the system, which is validated in real-time over an embedded system. The paper is organized as follows: in section II the mathematical modeling of the Boost converter and the

modified PID controller is presented. In section III, the discrete HIL implementation of the DC-DC Boost converter and the modified PID controller is presented, and finally, in section IV is presented the obtained results for simulated and HIL implementation over the embedded system.

II. DC-DC BOOST CONVERTER

Consider a simplified model of a DC-DC Boost converter presented in Fig. 1.

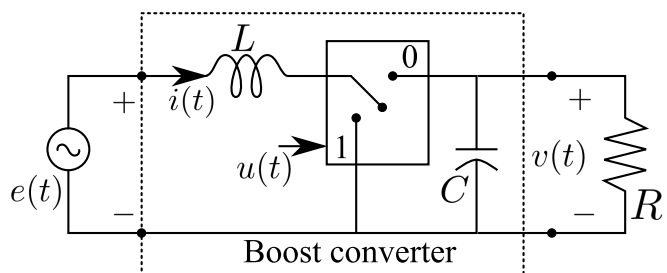


Fig. 1. Simplified Boost converter schematic circuit

This circuit can be modeled by the set of state-space equations (1) proposed in [11], as follows:

$$\begin{aligned} \dot{x}_1 &= -\omega_0 x_2(t) + u(t)\omega_0 x_2(t) + b(t) \\ \dot{x}_2 &= \omega_0 x_1(t) - \omega_1 x_2(t) - u(t)\omega_0 x_1(t) \end{aligned} \quad (1)$$

where $x_1(t) = i(t)\sqrt{L}$, $x_2(t) = v(t)\sqrt{C}$ are the normalized state-space variables of the inductor L input current $i(t)$ and the output capacitor C voltage $v(t)$, respectively. The variable $b(t) = \frac{e(t)}{\sqrt{L}} > 0$ is the normalized external voltage source $e(t)$. The constants $\omega_0 = \frac{1}{\sqrt{LC}}$ and $\omega_1 = \frac{1}{RC}$ are the natural undamped frequencies of the LC input circuit and the RC output circuit, respectively. Besides, $u(t)$ is the control signal related to the switch position with only two possible values $\{0, 1\}$.

The average model of the Boost converter of (1), by considering a Pulse-Width-Modulated (PWM) $u(t)$ signal, can be defined as

$$\begin{aligned} \dot{z}_1 &= -\omega_0 z_2(t) + \mu(t)\omega_0 z_2(t) + b(t) \\ \dot{z}_2 &= \omega_0 z_1(t) - \omega_1 z_2(t) - \mu(t)\omega_0 z_1(t) \end{aligned} \quad (2)$$

being $z_1(t)$ the average normalized input current, and z_2 the average normalized output voltage. It is worth noting that the discontinuous control input $u(t)$ of (1) is replaced by the continuous function $\mu(t)$ which is the duty cycle of the PWM, defined as $0 \leq \mu(t) \leq 1$.

The equilibrium point of the variables z_{10} and μ_0 around a normalized output constant voltage z_{20} and b_0 can be obtained as follows

$$\begin{aligned} 0 &= -\omega_0 z_{20} + \mu_0 \omega_0 z_{20} + b_0 \\ 0 &= \omega_0 z_{10} - \omega_1 z_{20} - \mu_0 \omega_0 z_{10} \end{aligned} \quad (3)$$

Manuscript received March 30, 2021; revised August 9, 2021. This work was carried out under the funding of the Universidad Tecnológica de Pereira, Vicerrectoría de Investigación, Innovación y Extensión. Research project: 6-20-7 "Estimación Dinámica de estados en sistemas multivariables acoplados a gran escala".

Eduardo Giraldo is a Full Professor at the Department of Electrical Engineering, Universidad Tecnológica de Pereira, Pereira, Colombia. Research group in Automatic Control. E-mail: egiraldo@utp.edu.co.

where μ_0 is obtained from (3) as

$$\mu_0 = \frac{\omega_0 z_{20} - b_0}{\omega_0 z_{20}} \quad (4)$$

and z_{10} is obtained as from (3) as

$$z_{10} = \frac{\omega_1 z_{20}}{\omega_0 - \mu_0 \omega_0} \quad (5)$$

Around the operational point $\mu_0, z_{10}, z_{20}, b_0$, the nonlinear system (2) is linearized as follows

$$\begin{aligned} \Delta \dot{z}_1 &= (\mu_0 - 1)\omega_0 \Delta z_2(t) + \omega_0 z_{20} \Delta \mu(t) \\ \Delta \dot{z}_2 &= (\omega_0 - \mu_0 \omega_0) \Delta z_1(t) - \omega_1 \Delta z_2(t) - \omega_0 z_{10} \Delta \mu(t) \end{aligned} \quad (6)$$

And by applying Laplace transform over (6) the following equations are obtained

$$\Delta Z_1(s) = \frac{-(1 - \mu_0)\omega_0 \Delta Z_2(s) + \omega_0 z_{20} \Delta \mu(s)}{s} \quad (7)$$

and

$$\Delta Z_2(s) = \frac{(1 - \mu_0)\omega_0 \Delta Z_1(s) - \omega_0 z_{10} \Delta \mu(s)}{s + \omega_1} \quad (8)$$

and by considering that $\Delta Z_2(s)$ is the output to be controlled, from (7) and (8) the following equation can be obtained

$$\begin{aligned} \Delta Z_2(s) &= \frac{-(1 - \mu_0)^2 \omega_0^2 \Delta Z_2(s) + (1 - \mu_0)\omega_0^2 z_{20} \Delta \mu(s)}{s(s + \omega_1)} \\ &\quad - \frac{\omega_0 z_{10} \Delta \mu(s)}{s + \omega_1} \end{aligned} \quad (9)$$

and from (9) the following transfer function can be obtained

$$\Delta Z_2(s) = \frac{-\omega_0 z_{10} s + (1 - \mu_0)\omega_0^2 z_{20}}{s^2 + \omega_1 s + (1 - \mu_0)^2 \omega_0^2} \Delta \mu(s) \quad (10)$$

The design criteria for the controllers is a fixed settling time t_s and a steady-state error equal to zero for an unitary step reference signal. To this end, a PID controllers is selected. Since (10) is a transfer function which includes a non-minimum phase zero at $s = \frac{(1 - \mu_0)\omega_0 z_{20}}{z_{10}}$, a modified structures of PID controller is used without increasing the system closed loop zeros. The PID structure is defined to have a control signal as

$$\begin{aligned} \Delta \mu(t) &= K_i \int (\Delta r(\tau) - \Delta z_2(\tau)) \delta \tau \\ &\quad - K_p \Delta z_2(t) - K_d \Delta \dot{z}_2(t) \end{aligned} \quad (11)$$

being K_p, K_d and K_i the controller constants. In Fig. 2 is shown the structure of the controller.

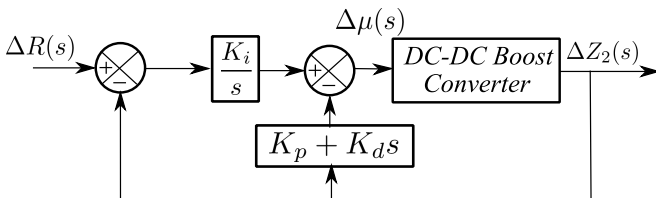


Fig. 2. Modified PID controller structure over DC-DC Boost converter

From Fig. 2 the following closed loop equation is obtained

$$\begin{aligned} \Delta Z_2(s) &= \frac{-\omega_0 z_{10} s + (1 - \mu_0)\omega_0^2 z_{20}}{s^2 + \omega_1 s + (1 - \mu_0)^2 \omega_0^2} \\ &\quad \left(\frac{K_i}{s} (\Delta R(s) - \Delta Z_2(s)) - (K_p + K_d s) \Delta Z_2(s) \right) \end{aligned} \quad (12)$$

which can be rewritten as

$$\begin{aligned} \Delta Z_2(s) &= \frac{c_1 s + c_2}{s^2 + c_3 s + c_4} \\ &\quad \left(\frac{K_i}{s} (\Delta R(s) - \Delta Z_2(s)) - (K_p + K_d s) \Delta Z_2(s) \right) \end{aligned} \quad (13)$$

being

$$c_1 = -\omega_0 z_{10} \quad (14)$$

$$c_2 = (1 - \mu_0)\omega_0^2 z_{20} \quad (15)$$

$$c_3 = \omega_1 \quad (16)$$

$$c_4 = (1 - \mu_0)^2 \omega_0^2 \quad (17)$$

Therefore, the closed loop system of (13) can be rewritten as

$$\Delta Z_2(s) = \frac{K_i c_1 s + K_i c_2}{P_{CL}(s)} \Delta R(s) \quad (18)$$

being the closed-loop polynomial equation $P_{CL}(s)$ defined by

$$\begin{aligned} P_{CL}(s) &= (1 + c_1 K_d) s^3 + (c_3 + K_d c_2 + K_p c_1) s^2 \\ &\quad + (c_4 + c_2 K_p + K_i c_1) s + K_i c_2 \end{aligned} \quad (19)$$

By considering a $P_{CL}(s)$ stable, then, the steady-state error can be computed as

$$e_{ss} = \lim_{s \rightarrow 0} s (\Delta R(s) - \Delta Z_2(s)) \quad (20)$$

being $\Delta R(s) = \frac{1}{s}$, resulting in

$$e_{ss} = 1 - \frac{K_i c_2}{K_i c_2} \quad (21)$$

where the $e_{ss} = 0$. It is worth noting that the values of K_p, K_i and K_d are independent of the steady-state error, therefore, the selection of controller parameters are computed based on the settling-time. By considering that the settling-time t_s can be related to the real magnitude of the dominant pole p , as follows

$$t_s \approx \frac{4}{p} \quad (22)$$

Therefore, the desired polynomial equation in closed loop must have a dominant pole at $s = -p$, if the pole is real or a dominant complex poles $s_{1,2} = -p \pm j\omega_d$, being ω_d the damped frequency. The desired closed loop polynomial is defined as

$$P_D(s) = s^3 + \alpha_1 s^2 + \alpha_2 s + \alpha_3 \quad (23)$$

Finally, the resulting equations system for $P_D(s) = P_{CL}(s)$ is obtained by

$$\begin{bmatrix} K_p \\ K_i \\ K_d \end{bmatrix} = \begin{bmatrix} c_1 & 0 & c_2 - \alpha_1 c_1 \\ c_2 & c_1 & -\alpha_2 c_1 \\ 0 & c_2 & -\alpha_3 c_1 \end{bmatrix}^{-1} \begin{bmatrix} \alpha_1 - c_3 \\ \alpha_2 - c_4 \\ \alpha_3 \end{bmatrix} \quad (24)$$

III. HIL IMPLEMENTATION OF THE BOOST CONVERTER

The discrete implementation of the DC-DC Boost converter is developed by using the structure depicted in Fig. 3, where an ARDUINO DUE based on a 32-bit ARM core microcontroller is used. The microcontroller includes 54 digital input/output pins, 12 analog inputs, 2 DAC, and a 84 MHz clock.

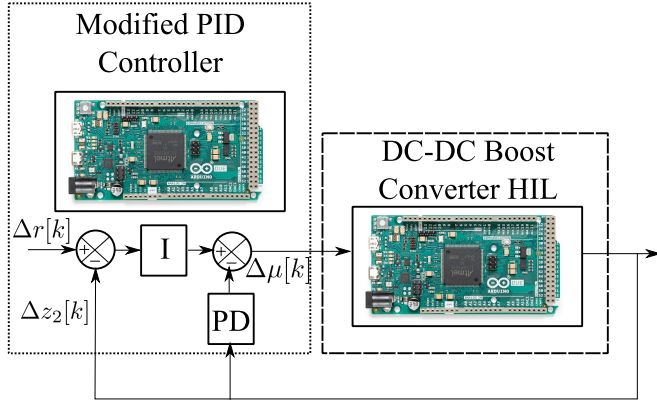


Fig. 3. Real time implementation of the modified PID controller over a DC-DC Boost converter

The modified PID controller in discrete time is computed by

$$\Delta e[k] = \Delta r[k] - \Delta z_2[k] \quad (25)$$

$$e_i[k] = e_i[k-1] + h\Delta e[k] \quad (26)$$

$$y_d[k] = \frac{\Delta z_2[k] - \Delta z_2[k-1]}{h} \quad (27)$$

$$u[k] = -K_p\Delta z_2[k] - K_d y_d[k] + K_i e_i[k] \quad (28)$$

being $y_d[k]$ the derivative of the output $\Delta z_2[k]$, $e_i[k]$ the integral of the error $\Delta e[k]$.

IV. RESULTS

In order to evaluate the performance of the controller, the following values are considered $E = 1V$, $L = 0.01H$, $C = 0.0001F$, $R = 1000\Omega$, and where the nonlinear model is approximated to a linear model around $z_{20} = 3V$. By considering these values, the following transfer function from (10) is obtained

$$\Delta Z_2(s) = \frac{-9000s + 10000}{s^2 + 10s + 11.1} \Delta \mu(s) \quad (29)$$

In Fig. 4 is presented the impulse response of the linearized DC-DC Boost converter (29).

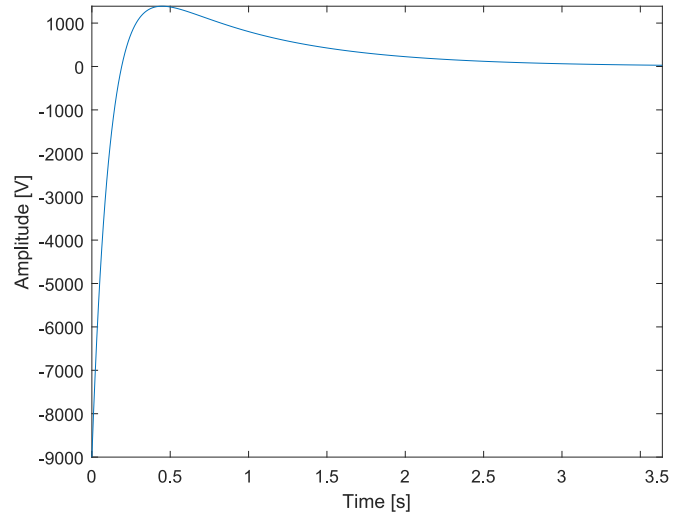


Fig. 4. Impulse response of (29)

It is worth noting that (29) has a non-minimum phase zero, resulting in a large undershoot, which increase the difficulty of the control design. This can be verified by analyzing the step response presented in Fig. 5.

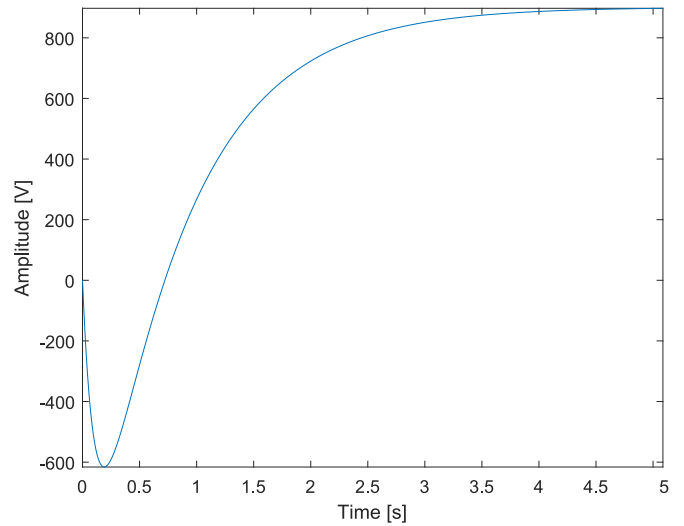


Fig. 5. Step response of (29)

However, by considering a settling-time $t_s = 4$ seconds, as dominant dynamics, while holding the independent coefficient as smallest as possible, the following desired equation is obtained:

$$P_D(s) = (s+1)(s+4)^2 \quad (30)$$

$$P_D(s) = s^3 + 9s^2 + 24s + 16 \quad (31)$$

and by considering (24) and (30), the following equation is obtained

$$\begin{bmatrix} K_p \\ K_i \\ K_d \end{bmatrix} = \begin{bmatrix} 7.0363 \times 10^{-4} \\ 7.5614 \times 10^{-4} \\ 5.8601 \times 10^{-5} \end{bmatrix} \quad (32)$$

and therefore (13) is given by (33), as follows

$$\Delta Z_2(s) = \frac{-6.805s + 7.561}{0.4726s^3 + 4.253s^2 + 11.34s + 7.561} \Delta R(s) \quad (33)$$

In Fig. 6 is shown the unitary impulse response of (33).

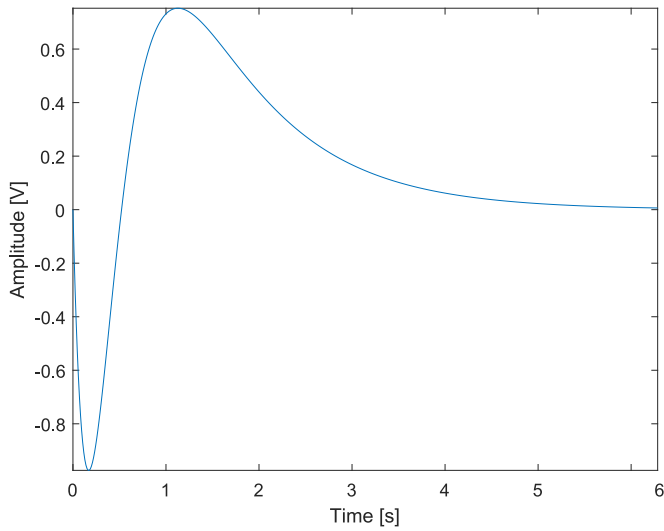


Fig. 6. Unitary impulse response of (33)

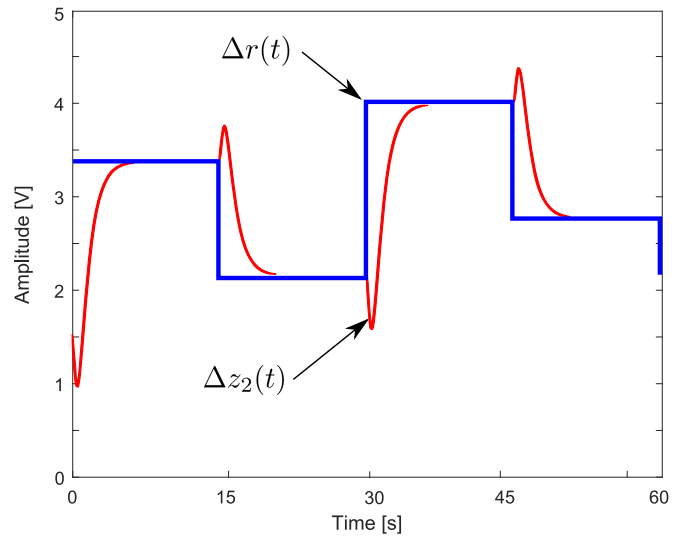


Fig. 8. Closed loop response for small variations around operational point

In Fig. 7 is shown the unitary step response of (33).

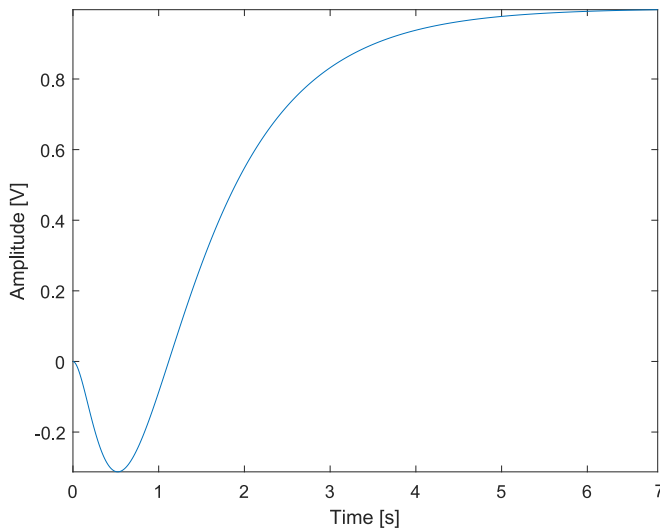


Fig. 7. Unitary step response of (33)

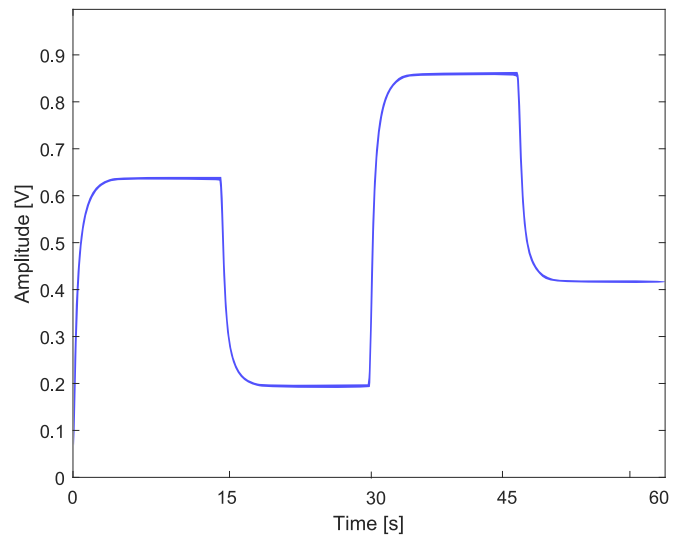


Fig. 9. Control signal $\Delta\mu(t)$ for test of Fig. 8

Another trial including 60 seconds of simulation time with small variations around the 120V is presented in Fig. 10.

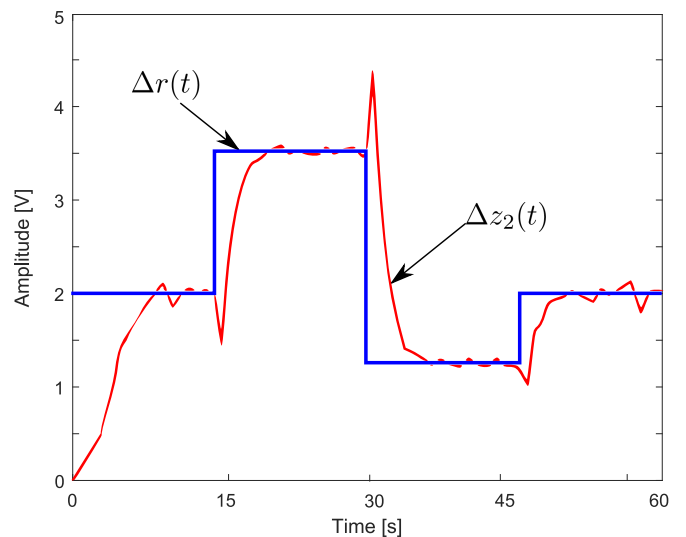


Fig. 10. Closed loop response for small variations around 120V

It is worth noting that in Fig. 4 in comparison with Fig. 7, a reduction in the non-minimum phase zero effect is obtained. A detailed trial including 60 seconds of simulation time with small variations around the operational point is presented in Fig. 8.

The corresponding control signal $\Delta\mu(t)$ is shown in Fig. 11.

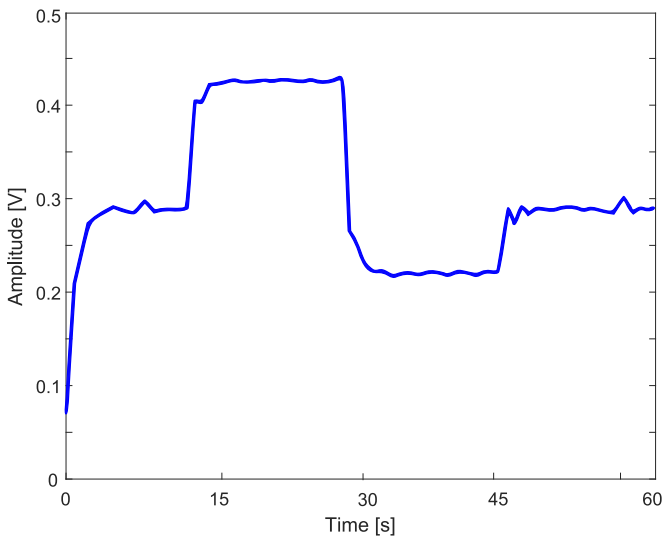


Fig. 11. Control signal $\Delta\mu(t)$ for test of Fig. 10

A parametric modification of the system is developed by considering a DC-DC Boost converter with the following values $E = 2V$, $L = 0.00001H$, $C = 0.001F$, $R = 10\Omega$, and where the nonlinear model is approximated to a linear model around $z_{20} = 3V$. By considering these values, the following transfer function from (10) is obtained as follows

$$\Delta Z_2(s) = \frac{-14230s + 6324555}{s^2 + 100s + 44444} \Delta\mu(s) \quad (34)$$

In Fig. 12 is presented the impulse response of the linearized DC-DC Boost converter (34).

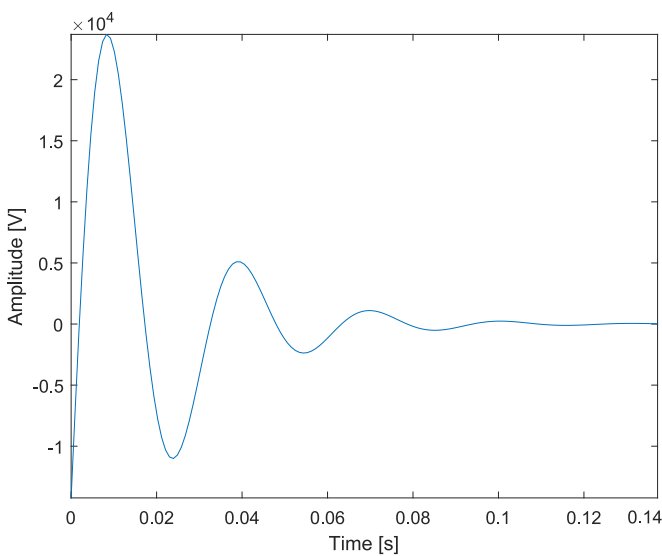


Fig. 12. Impulse response of (34)

In Fig. 13 is presented the step response of the linearized DC-DC Boost converter (34).

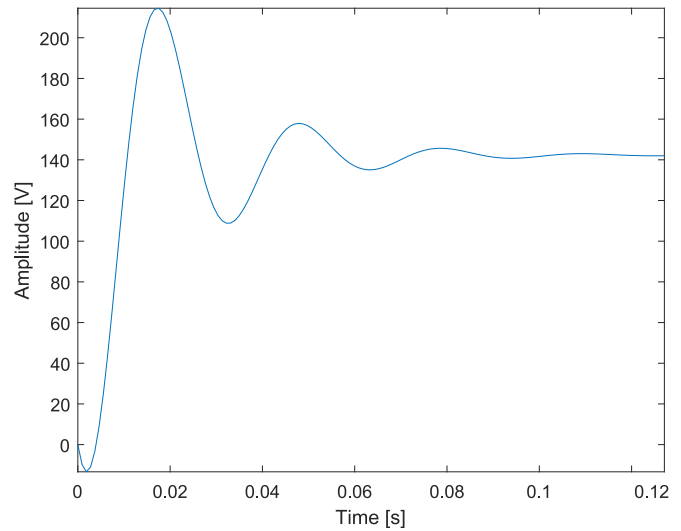


Fig. 13. Step response of (34)

By considering a settling-time $t_s = 1$ seconds, as dominant dynamics, while holding the independent coefficient as smallest as possible, the following desired equation is obtained:

$$P_D(s) = (s + 4)(s + 16)^2 \quad (35)$$

$$P_D(s) = s^3 + 36s^2 + 384s + 1024 \quad (36)$$

and by considering (24) and (35), the following equation is obtained

$$\begin{bmatrix} K_p \\ K_i \\ K_d \end{bmatrix} = \begin{bmatrix} -0.00694 \\ 2.1678 \times 10^{-4} \\ -2.3817 \times 10^{-5} \end{bmatrix} \quad (37)$$

and therefore (13) is given by (38), as follows

$$\Delta Z_2(s) = \frac{-3.085s + 1371}{1.339s^3 + 48.2s^2 + 514.1s + 1371} \Delta R(s) \quad (38)$$

In Fig. 14 is shown the unitary impulse response of (38).

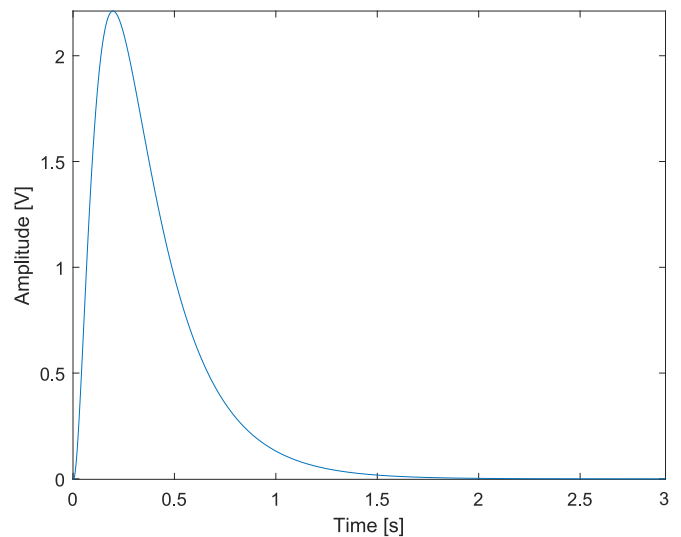


Fig. 14. Unitary impulse response of (38)

In Fig. 15 is shown the unitary step response of (38).

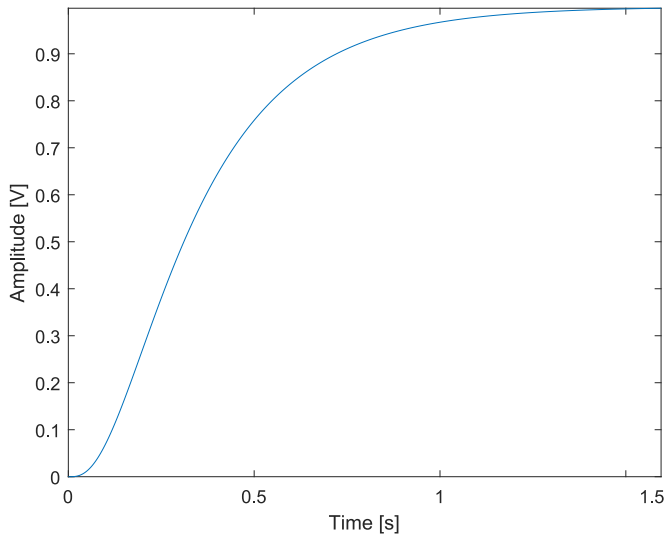


Fig. 15. Unitary step response of (38)

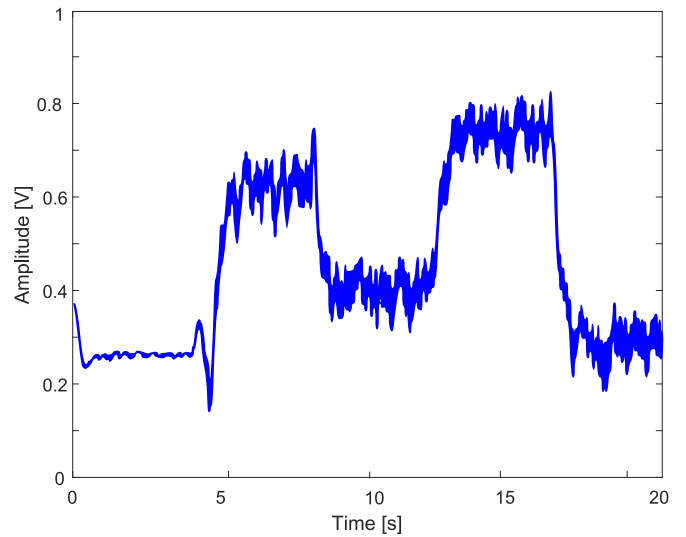


Fig. 17. Control signal $\Delta\mu(t)$ for test of Fig. 16

By considering 20 seconds of HIL simulation time with small variations around the operational point z_{20} , the closed loop response is depicted in Fig. 16.

By considering 5 seconds of HIL simulation time with step reference signal variation around the operational point z_{20} , the closed loop response is depicted in Fig. 18.

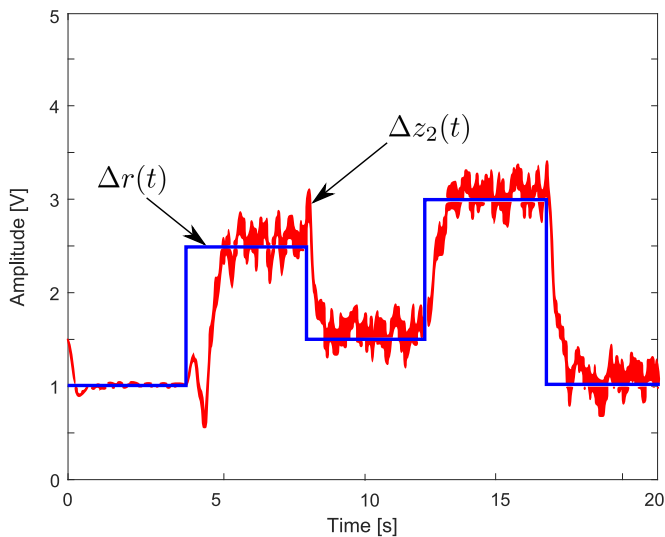


Fig. 16. Closed loop response for small variations around z_{20}

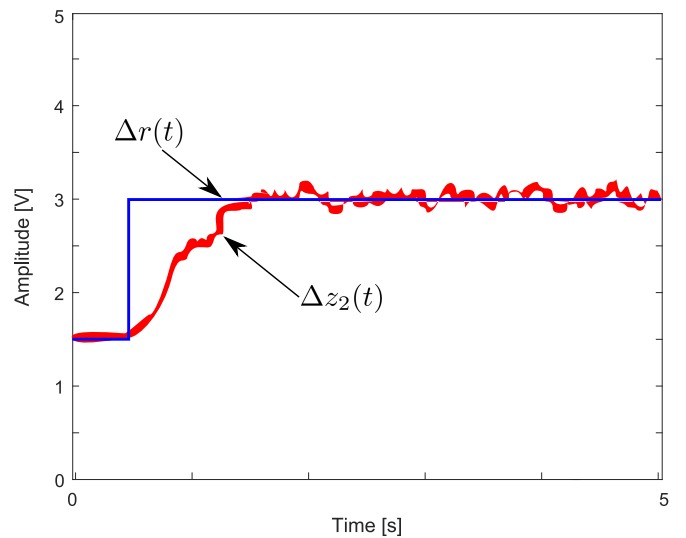


Fig. 18. Closed loop response for small step reference variation around z_{20}

The corresponding control signal $\Delta\mu(t)$ is shown in Fig. 17.

Finally, by considering 5 seconds of HIL simulation time with impulse reference signal variation around the operational point z_{20} , the closed loop response is depicted in Fig. 19.

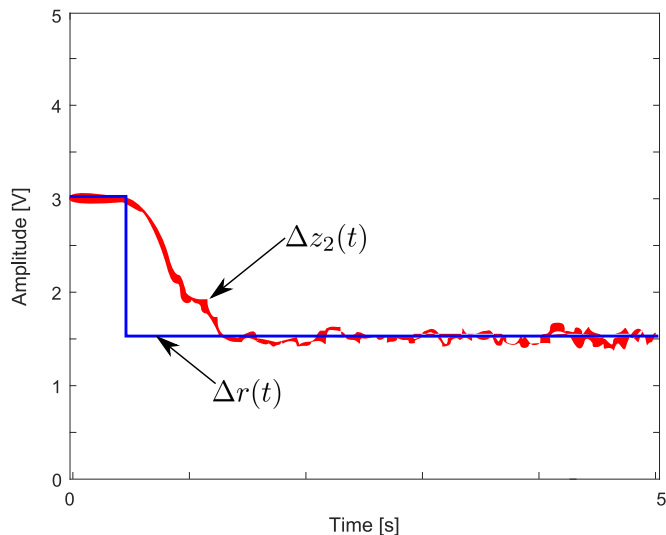


Fig. 19. Closed loop response for small impulse reference variation around z_{20}

V. CONCLUSIONS

In this work, a real-time evaluation of a modified PID controller is developed. The controller is designed by considering the settling time and a non-minimum phase system corresponding to a linearized DC-DC Boost converter. The designed PID is applied over a DC-DC Boost converter in simulation and by using a HIL structure for real-time analysis. As presented in section IV, the proposed approach improves the performance of the closed-loop system for tracking references with a reduction of the undershoot, which is an inherent feature of non-minimum phase systems. Also, the method is validated by considering parametric variations and two settling time conditions. The HIL structure shows the tracking performance of the proposed method for real reference signal variations around the operational point, such as step and impulse reference signals. Finally, it is worth mentioning that the HIL validation in real-time of the proposed approach improves

the results over real conditions, which is a required stage for rapid prototyping. As future works, the fractional-order PI controllers can be designed and evaluated in real-time over DC-DC converters.

REFERENCES

- [1] A. Samiee, N. Tiefnig, J. P. Sahu, M. Wagner, A. Baumgartner, and L. Juhász, "Model-driven-engineering in education," in *2018 18th International Conference on Mechatronics - Mechatronika (ME)*, 2018, pp. 1–6.
- [2] F. Osorio-Arteaga, J. J. Marulanda-Durango, and E. Giraldo, "Robust multivariable adaptive control of time-varying systems," *IAENG International Journal of Computer Science*, vol. 47, no. 4, pp. 605–612, 2020.
- [3] C. A. Ramirez-Vanegas and E. Giraldo, "Real-time implementation of a discrete fractional-order pid control," *IAENG International Journal of Computer Science*, vol. 48, no. 1, pp. 50–56, 2021.
- [4] G. A. Korn, "Continuous-system simulation and analog computers: from op-amp design to aerospace applications," *IEEE Control Systems Magazine*, vol. 25, no. 3, pp. 44–51, 2005.
- [5] J. J. Marulanda-Durango, A. Escobar-Mejia, and E. Giraldo, "Multivariable coupled control of a static var compensator to improve the power factor of a steel plant with an electric arc furnace load," *Engineering Letters*, vol. 29, no. 2, pp. 365–372, 2021.
- [6] J. S. Velez-Ramirez, L. A. Rios-Norena, and E. Giraldo, "Buck converter current and voltage control by exact feedback linearization with integral action," *Engineering Letters*, vol. 29, no. 1, pp. 168–176, 2021.
- [7] J. S. Velez, S. Ospina, and E. Giraldo, "Passivity-based control for a buck-boost converter applied in small wind generation interconnected to dc microgrid," in *2019 IEEE 4th Colombian Conference on Automatic Control (CCAC)*, 2019, pp. 1–6.
- [8] G. A. Ramos, M. E. Hernández, and M. D. Trujillo, "Function test by hil for dc-dc converters type: Buck, boost and buck-boost," in *2017 IEEE Workshop on Power Electronics and Power Quality Applications (PEPQA)*, 2017, pp. 1–6.
- [9] A. H. R. Rosa, L. M. F. Morais, and I. S. Seleme, "Hardware in the loop simulation of non linear control methods applied for power converters," in *2015 IEEE 13th Brazilian Power Electronics Conference and 1st Southern Power Electronics Conference (COBEP/SPEC)*, 2015, pp. 1–6.
- [10] B. Lu, X. Wu, H. Figueroa, and A. Monti, "A low-cost real-time hardware-in-the-loop testing approach of power electronics controls," *IEEE Transactions on Industrial Electronics*, vol. 54, no. 2, pp. 919–931, 2007.
- [11] H. Sira-Ramirez, R. Marquez, F. Rivas-Echeverria, and O. Llanes-Santiago, *Control de Sistemas No Lineales*. Prentice-Hall, Pearson Education, 2004.